Progress In Electromagnetics Research C, Vol. 88, 89–101, 2018

Design of A Novel Low-Cost High-Gain Dual-Polarized Antenna by Suspended Cylinder and Shorting Strips

Subash C. Yadav* **and Siddhartha P. Duttagupta**

Abstract—In this paper, a novel low-cost, high gain dual-polarized antenna design with a suspended cylinder and a ground connected cylinder geometry is proposed. The design structure of the antenna is simple and fabricated with two cylinders, two shorting strips, and a circular ground plane. All these components are easily fabricated from a copper sheet of thickness 0.4 mm, and the antenna is fed by two coaxial probes at the orthogonal planes on the circumference of the cylinders. A prototype is designed, fabricated and measured. The measured results show that the prototype has −10 dB impedance bandwidth of 34.37% at port 1 & 34.21% at port 2. Broadside gain from port 1 is 10.2–10.4 dBi & port 2 is 10.25–10.52 dBi, which indicates that the antenna has flat gain over the impedance bandwidth, and isolation between the ports is more than 15 dB from 2.65-3.6 GHz and more than 20 dB from 2.75–3.55 GHz. The isolation of the proposed antenna is improved by shorting the suspended cylinder to the ground plane by two shorting strips. The resonance frequency and isolation peak are simultaneously tunable with varying the width of the shorting strips. The parameters of the antenna are optimized by using HFSS, and good agreement between the simulated and measured results is obtained. The proposed dual polarized antenna can be used for base station applications such as LTE (Long Term Evolution) and WiMAX (Worldwide Interoperability for Microwave Access).

1. INTRODUCTION

One of the key components in the wireless mobile communication system is the base station antenna, which plays an important role to transmit and receive the electromagnetic wave in free space [1]. With the rapid growth of mobile communication systems, the base station antennas with wide bandwidth, high unidirectional gain, and stable radiation pattern are in demand and have received intensive study [2, 3]. Dual polarized antennas are widely used because they can reduce multipath fading, improve channel capacity, double the utilization rate of frequency spectrum and reduce installation costs [4, 5]. Moreover, low-cost, simple structure, simple feeding, and easily fabricable antennas are preferred. The dual-polarized antenna reported in [6] has impedance bandwidth of 1.5–3.9 GHz with peak gain of 8.7 dBi, and isolation between the ports is more than 30 dB, but antenna design required impedance matching network as baluns; however, components such as reflector, spacer, dipole, crossfeed lines, and dielectric material are used in the fabrication which increases the cost and complexity of the antenna. The dual polarized patch antenna reported in [7] required two separate patches for two different polarizations, with two parasitic elements, a feeding network, and an absorber is used to provide the isolation between the ports; therefore, antenna cost and complexity are increased. However, the dual polarized antenna reported in [8] has impedance bandwidth of 0.75–1 GHz with the peak gain of 10.2 dBi, and isolation is more than 26 dB, but antenna design required 4 baluns, feeding pads, base reflector, metal reflector, 4 dipoles, and dielectric-filled cables. With all these components the antenna cost and complexity are increased. The dual polarized antennas reported in [9–11] required external feeding networks, and a

Received 8 September 2018, Accepted 26 October 2018, Scheduled 7 November 2018
* Corresponding author: Subash C. Yadav (subashiitkgp@gmail.com).
The authors are with the Department of Electrical Engineering, IIT Bombay, India.

large number of components are used for fabrication, which creates design complexity and increases the fabrication cost.

In the aforementioned designs, most of them reported that dual polarized antennas require a complex feeding network and antenna structure since they use a large number of components for fabrication. In order to address the complexity issue, we propose an extremely low-cost high gain dual polarized antenna having a simple structure and fabricated using metal. It is fed using two orthogonal coaxial probes and thus does not require any external feeding network, and the same antenna generates vertical and horizontal polarizations when being fed from port 1 and port 2, respectively. Figure 1 shows the design structure of the proposed antenna, and here a suspended cylinder, a ground connected cylinder, two shorting strips, and a circular ground plane are used. The shorting strips enhanced the port isolation by shorting the suspended cylinder from the ground plane. The location of strip 1 made $\pm 180^\circ$ from port 1, and strip 2 made $\pm 180^\circ$ from port 2 on the circumference of the cylinders. The resonance frequency and isolation peak are simultaneously tunable with the width of the shorting strips. The simulated antenna of the resonance frequency, 2.95 GHz, has -10 dB impedance bandwidth of 32.25% (2.6–3.6 GHz) with isolation more than 15 dB, and broadsides gain is 10.8 ± 0.1 dBi over the entire bandwidth. The simulated isolation between the ports is more than 20 dB over -15 dB impedance bandwidth of 18.87% (2.75–3.32 GHz). The simulated antenna has a symmetrical response with respect to port 1 and port 2. The antenna is fabricated and measured, and good agreements with simulated results are obtained. However, small deviation in measured results is found due to the fabrication tolerances and measurement errors.

2. DESIGN STRUCTURE

The structure of the proposed antenna is shown in Figure 1. It consists of a circular ground plane of radius R, a ground connects cylinder with outer radius 'b' and height 'H_1', a suspended cylinder with outer radius 'a' and height 'H_2'. The height of the coaxial probes from the ground plane is 'h', and 'w_1' is the height of the coaxial probe from the bottom point of the suspended cylinder. The suspended height of the cylinder and length of the shorting strips from the ground plane is 'H_3', and 'w' is the width of the shorting strips. The total height of the antenna from the ground plane is 'L', and the air gap between the cylinders is 'g'. The thickness of the cylinders, shorting strips and ground plane is

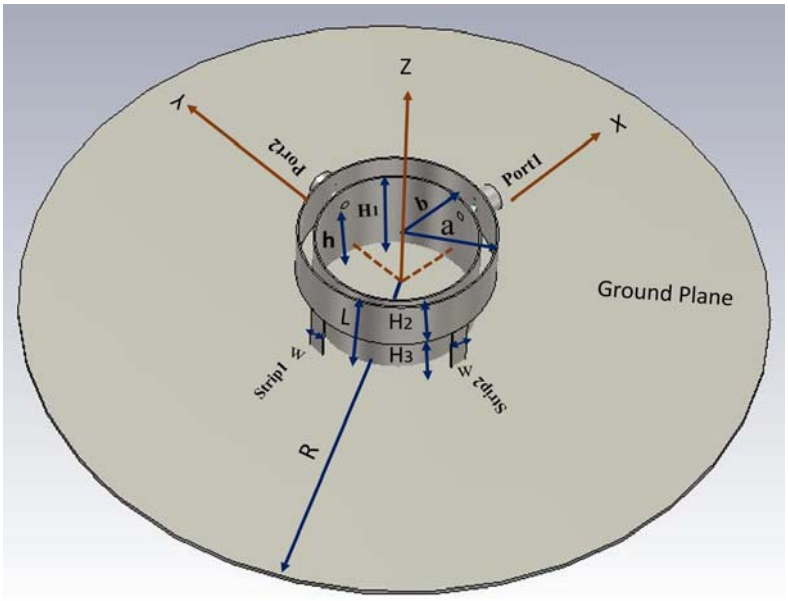

Figure 1. The design structure of the proposed dual polarized antenna with the suspended cylinder and shorting strips.

0.4 mm. The shorting strips are used to short the suspended cylinder to the ground plane to enhance the isolation between the ports. Strip1 made an angle ±180° from port 1, and strip 2 made an angle ±180° from port 2 on the circumference of the cylinders (The shorting strips and coaxial probes are opposite sides on the diagonal of the cylinders). All the dimensions are indicated in Figure 1, and its corresponding optimized values are mentioned in Table 1.

Table 1. The optimized dimensions of the proposed antenna in (mm).

R	H_1	H_2	h	b	a	L	w_1	H_3	w	g
80	22	12	17	17.8	21.4	24	5	12	4	3.2

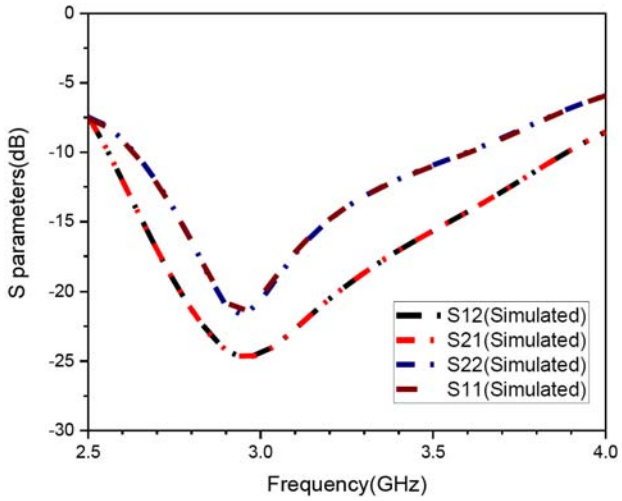

Figure 2. Simulated S parameters of the proposed antenna.

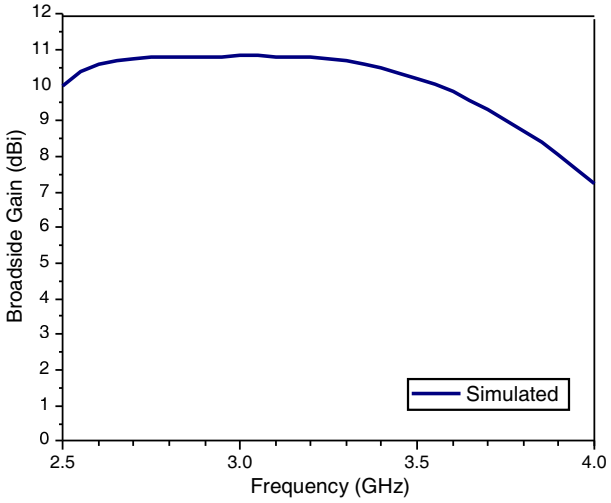

Figure 3. Simulated broadside gain of the proposed antenna.

The proposed antenna is simulated by taking dimensions from Table 1, and its scattering parameters and broadside gain are mentioned in Figure 2 and Figure 3, which show that the antenna has a symmetrical response with respect to ports. The simulated antenna has resonance frequency 2.95 GHz with an impedance bandwidth of 2.6–3.6 GHz. Isolation between the ports is 25 dB at the resonance frequency, more than 15 dB for 2.65–3.6 GHz, and more than 20 dB for 2.75–3.3 GHz. The simulated antenna has stable broadside radiation pattern with 10.8±0.1 dBi gain over the entire −10 dB impedance bandwidth.

3. DESIGN PROCEDURE

The structure of the antenna is shown in Figure 1, where the ground-connected cylinder and suspended cylinder are fed from two orthogonal coaxial probes at height 'h' from the ground plane. The antenna simulated without shorting strips has resonance frequency 2.65 GHz with −10 dB impedance 34.48% (2.4–3.4 GHz), and isolation between the ports is more than 10 dB over impedance bandwidth which is shown in Figure 4. The current distribution of the antenna without shorting strips is simulated when port 1 is excited and port 2 terminated with 50-ohm impedance, shown in Figure 6. Current distribution when port 2 is excited and port 1 terminated with 50-ohm impedance is shown in Figure 7. The current density vares across the circumference of the cylinders; therefore, resonance frequency of the antenna without shorting strips can be found mathematically by equating average circumference of cylinders to wavelength, but major component of the current is flowing across the circumference of the ground-connected cylinder, hence equating the circumference of ground-connected cylinder to wavelength gives

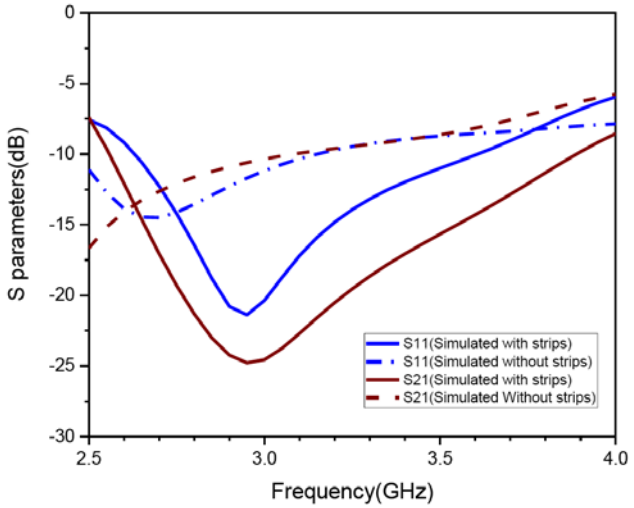

Figure 4. Simulated S parameters of the proposed antenna with and without strips.

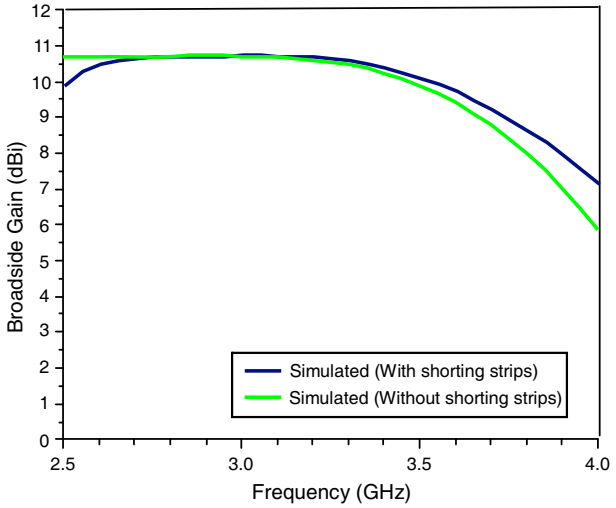

Figure 5. Simulated broadside gain of the proposed antenna with and without strips.

more accurate resonance frequency. There is strong electric field coupling between the cylinders which enhances the impedance bandwidth.

$$C_g \approx \lambda \quad \text{or} \quad fr \approx \frac{c}{c_g} \tag{1}$$

where C_g is the circumference of the ground connected cylinder, fr the resonance frequency, λ the wavelength corresponding to the resonance frequency, and c the speed of light in free space.

The simulated resonance frequency without shorting strips is 2.65 GHz whereas resonance frequency 2.68 GHz is obtained from Equation (1). The antenna simulated without shorting strips has poor isolation, which is more than 10 dB over impedance bandwidth, shown in Figure 4, and the antenna has flat broadside gain 10.7 dBi over the impedance bandwidth, shown in Figure 5.

However, the shorting strips are used to short the suspended cylinder and ground plane. Due to these shorting strips, some current flows from the suspended cylinder to the ground plane. Therefore, current coupling from port 1 to port 2 is reduced, hence the isolation between the ports is improved. The current flows from suspended cylinder to ground plane through the shorting strips; therefore, the shorting strips affect the inductive part of impedance as the strip width increases more current flow from the suspended cylinder to the ground plane. Thus, the inductive impedance of the strips is changed by varying the width. As a result, resonance frequency of the antenna is tunable by varying the width of shorting strips.

Hence, the resonance frequency of the antenna is shifted from 2.65 GHz to 2.95 GHz with the use of shorting strips with width $w = 4$ mm. The simulated antenna with shorting strips has resonance frequency 2.95 GHz with -10 dB impedance bandwidth (2.6–3.6 GHz), and the antenna has stable broadside gain (10.8 ± 0.1 dBi) over the entire bandwidth. The simulated current distributions of the proposed antenna with shorting strips are plotted at resonance frequency 2.95 GHz and are shown in Figure 8, and Figure 9, when port 1 and port 2 are excited, respectively. The simulated current density varies across the circumference of the cylinders; however, some current from the suspended cylinder is going to the ground plane through the strips. Therefore, shorting strips have some inductance, which changes the input impedance of the proposed antenna. As the strips width is varied, the inductance of the shorting strips varies; therefore, the resonance frequency of the antenna is tunable with strips' width. The electric field distribution of the antenna simulated at 2.95 GHz when port 1 is excited & port 2 terminated with 50-ohm, and when port 1 is terminated with 50-ohm & port excited and are shown in Figure 10 and Figure 11, respectively. When port 1 is excited, the major component of the electric field is along port 1 and orthogonal to port 2. When port 2 is excited, the major component of the electric field is along port 2 and orthogonal to the port 1. Therefore, horizontal polarization and vertical polarization are generated from port 1 and port 2.

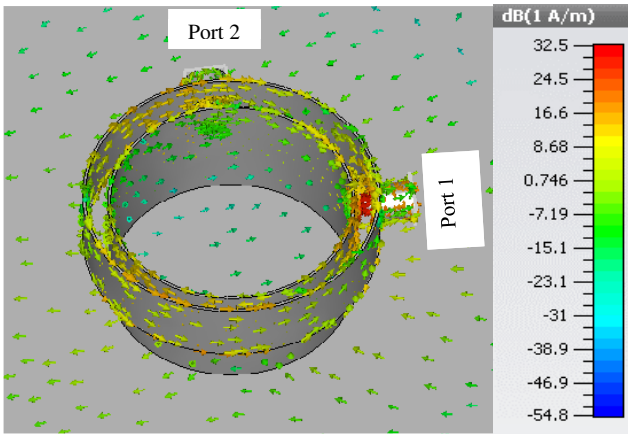

Figure 6. The simulated surface current density of the antenna without shorting strips at 2.65 GHz from port 1.

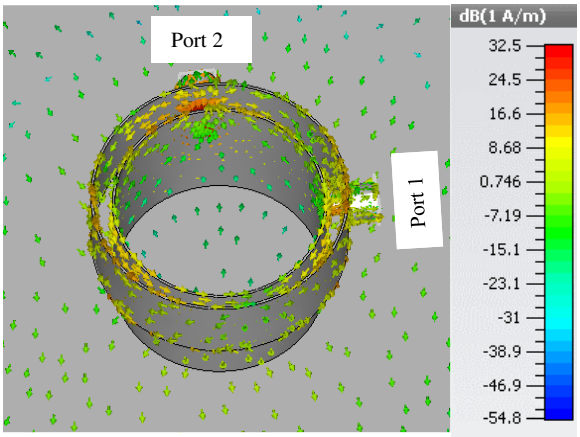

Figure 7. The simulated surface current density of the antenna without shorting strips at 2.65 GHz from port 2.

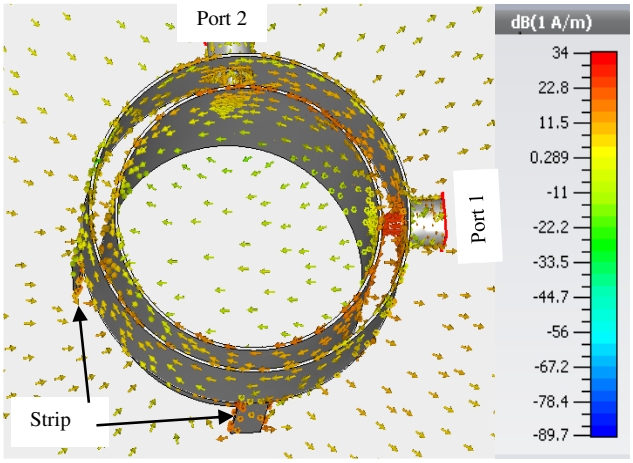

Figure 8. The simulated surface current density of the antenna with shorting strips at 2.95 GHz from port 1.

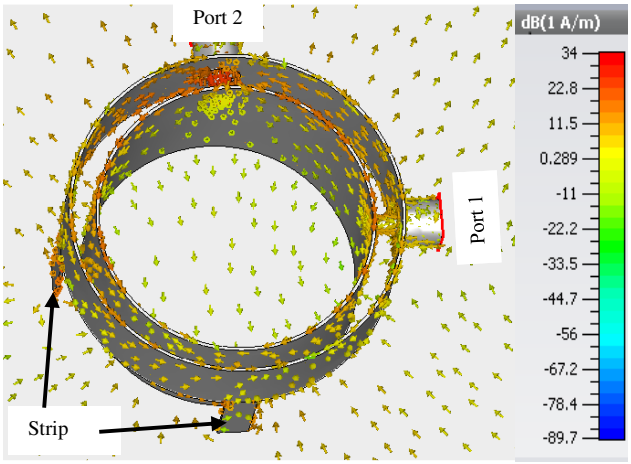

Figure 9. The simulated surface current density of the antenna with shorting strips at 2.95 GHz from port 2.

4. PARAMETRIC STUDY

In this section, the effect of antenna performance by changing antenna dimensions has been studied from the dimensions mentioned in Table 1. In this parametric study, at a time only one dimension of the antenna is varied, and corresponding effects on antenna performance are studied. The effects on the resonant frequency of the antenna by varying the shorting strips width are studied and shown in Figure 12, which shows that the resonance frequency is shifted to the right side by increasing the width of the strips. The isolation between the ports is shown in Figure 13, which shows that the isolation with shorting strips is improved, and isolation peak is shifted to the right side by increasing the width of the strips. The resonance frequency and isolation peak are simultaneously tunable with the change in strips width, and the antenna has isolation 25 dB at the resonance frequency. The antenna is tunable; therefore, 25 dB isolation can be achieved for any particular frequency over impedance bandwidth by tuning strip width. The broadside gain of the proposed antenna is simulated with different values of the strip width, and results are shown in Figure 14, which shows that the broadside gain of the antenna

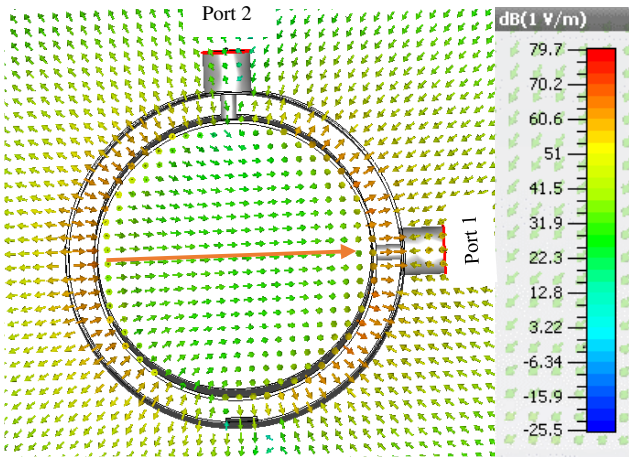

Figure 10. Simulated electric field distribution of the antenna with shorting strips at 2.95 GHz from port 1.

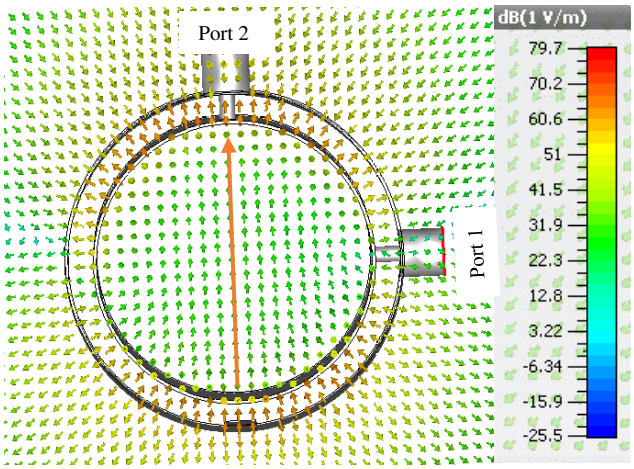

Figure 11. Simulated electric field distribution of the antenna with shorting strips at 2.95 GHz from port 2.

is also shifted to the right side by increasing the width of the shorting strips.

The effect of ground plane radius on the resonance frequency and impedance bandwidth has been studied and shown in Figure 15, which shows that there is a very small shift in resonance frequency with ground plane radius. The broadside gain of the antenna is simulated with a different ground plane radius. The result is shown in Figure 16, which shows that the broadside gain increases as the ground plane radius increases due to increase in effective area. In Figure 17, the effect of port isolation with ground plane radius is studied, and the result indicates that isolation peaks are shifted with ground plane radius. The effect of varying air gap between the cylinder on return loss and isolation is shown in Figure 18 and Figure 19 which indicates that the resonance frequency and isolation peaks are shifted to right side because we reduce inner cylinder radius to increase gap between the cylinders; therefore, the circumference of inner cylinder decreases which shifts the resonance frequency and isolation to the right side.

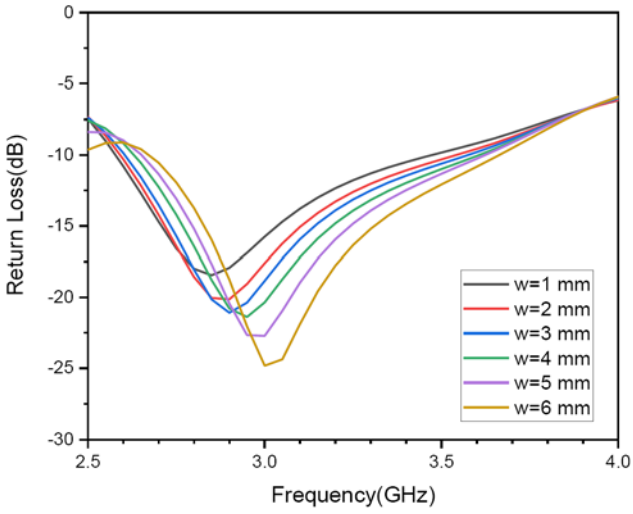

Figure 12. The simulated return loss of the proposed antenna with varying strips width.

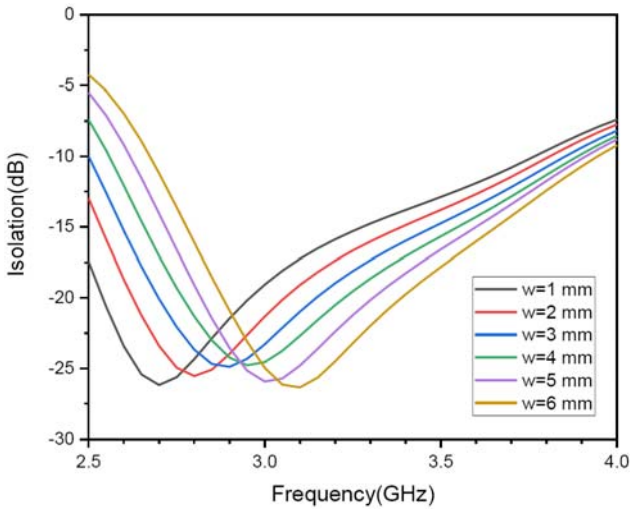

Figure 13. Simulated isolation of the proposed antenna with varying strips width.

5. FABRICATION AND MEASUREMENT RESULTS

The prototype of the proposed dual polarized antenna is shown in Figure 20, which is fabricated by taking dimension from Table 1. The design structure of the antenna is simple, and its all components such as cylinders, ground plane, and shorting strips are designed by the copper metal of thickness 0.4 mm. Two 50-ohm SMA connector is used to feed the antenna on orthogonal planes. The shorting strips are used to short the suspended cylinder to the ground plane. Strip 1 made $\pm 180^{\circ}$ from port 1, and strip 2 made $\pm 180^{\circ}$ from port 2 on the circumferences of the cylinders. The simulated and measured return losses from port 1 and port 2 are shown in Figure 21 and Figure 22, respectively . The simulated and measured isolations between the ports are shown in Figure 23, and simulated and measured broadside gains from port 1 and port 2 are shown in Figure 24. The measured bandwidth, isolation and broadside gain are mentioned in Table 2.

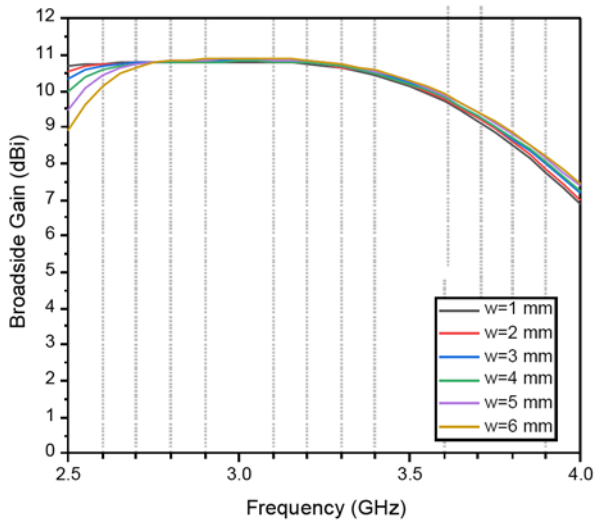

Figure 14. Simulated broadside gain of the proposed antenna with varying strips width.

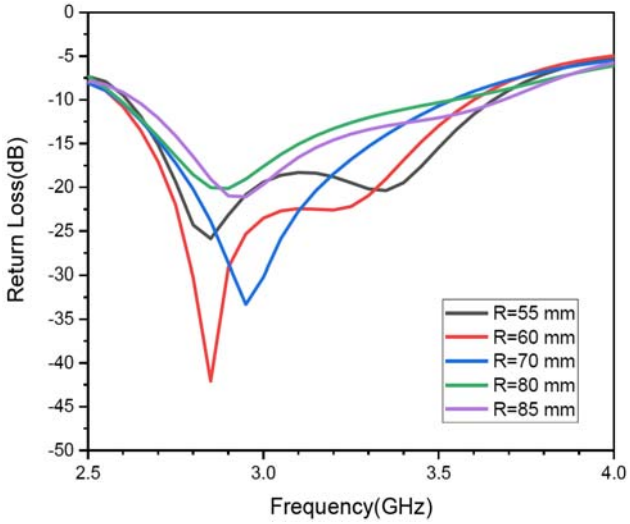

Figure 15. The simulated return loss of the proposed antenna with varying ground plane.

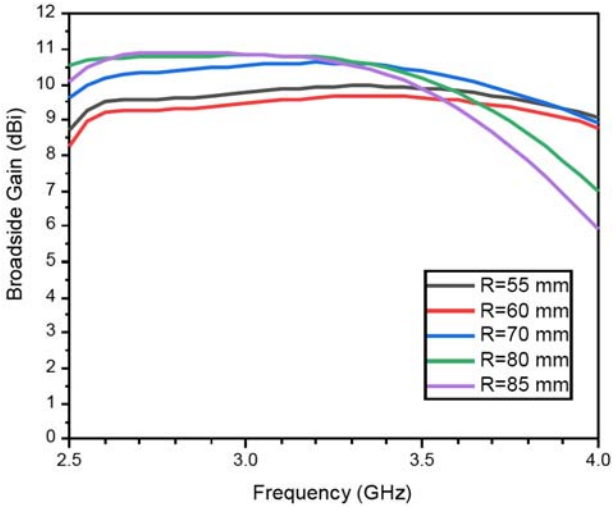

Figure 16. Simulated broadside gain of the proposed antenna with varying ground plane radius.

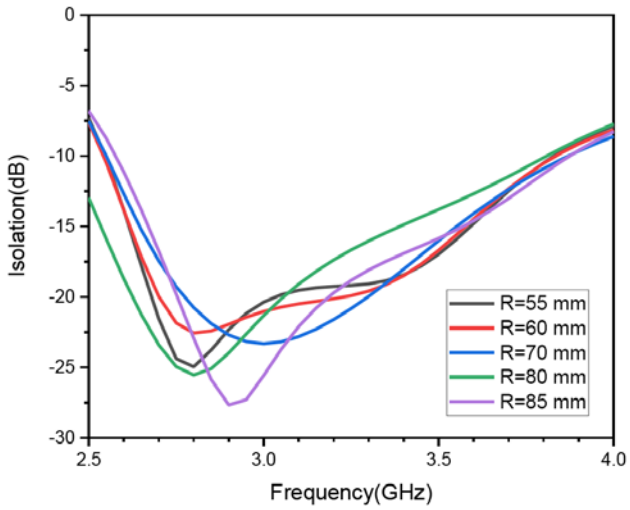

Figure 17. Simulated isolation of the proposed antenna with varying ground plane radius.

6. RESULTS AND DISCUSSIONS

The proposed antenna is simulated, fabricated and measured. The measurement and simulation results are mentioned in Table 2, which shows that the simulated antenna has symmetrical response from both the ports, and the antenna has −10 dB impedance bandwidth of 32.25% (2.6–3.6 GHz); however, the measurement shows that the antenna has impedance bandwidth of 34.37% (2.65–3.75 GHz) measured

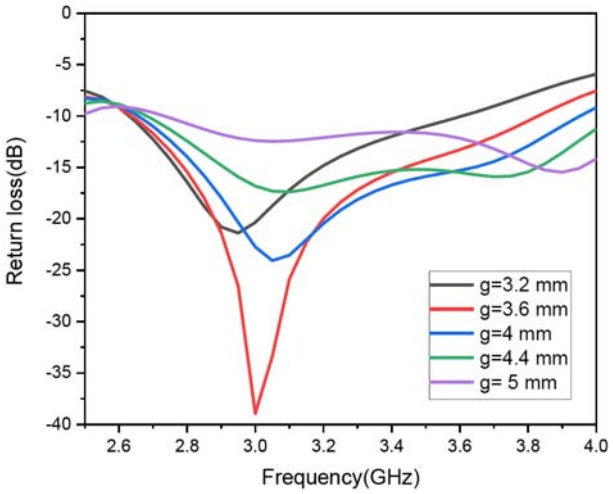

Figure 18. The simulated return loss of the proposed antenna with varying the gap between the cylinders.

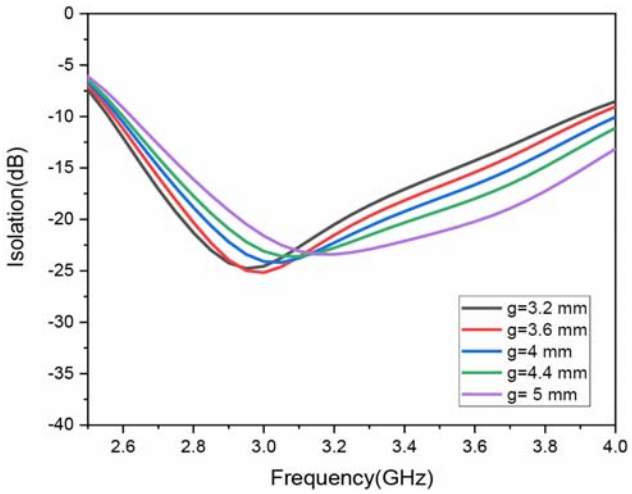

Figure 19. Simulated isolation between the ports by varying the gap between the cylinders.

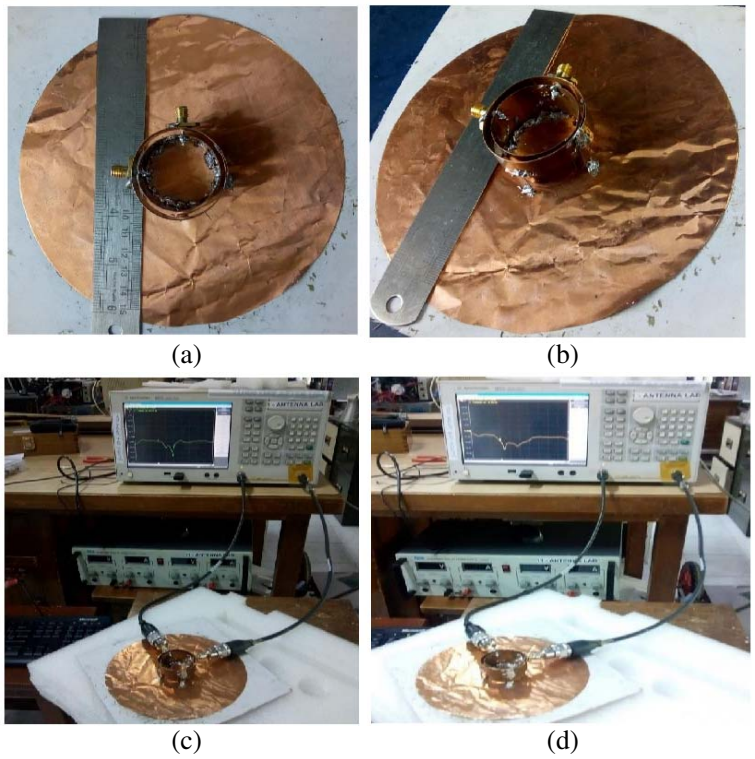

Figure 20. Prototype of the proposed dual polarized antenna. (a) Top view. (b) Side view. (c) Return loss measurement setup. (d) Isolation measurement setup.

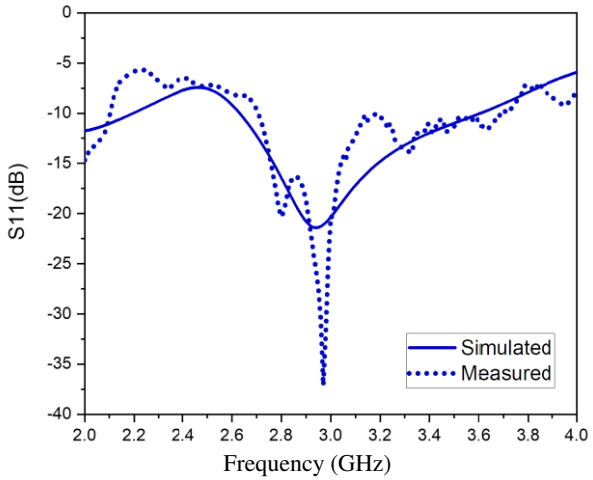

Figure 21. Comparison of simulated and measured return loss at port 1.

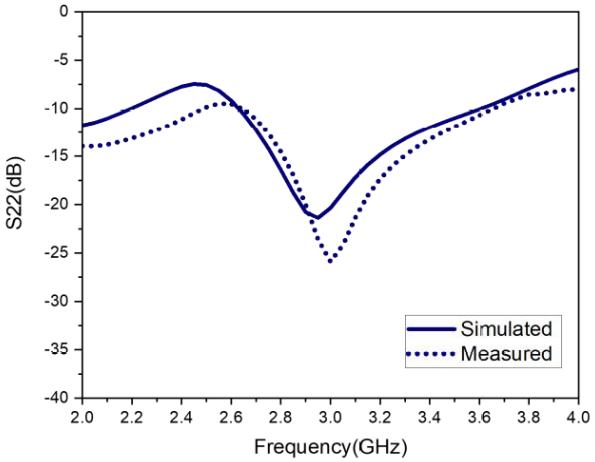

Figure 22. Comparison of simulated and measured return loss at port 2.

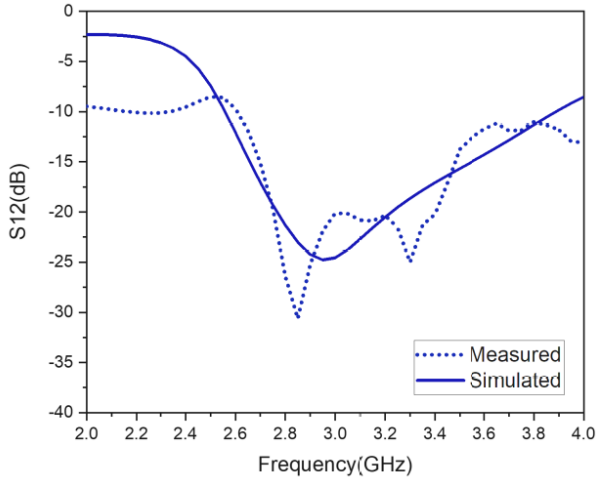

Figure 23. Comparison of simulated and measured isolation between the ports.

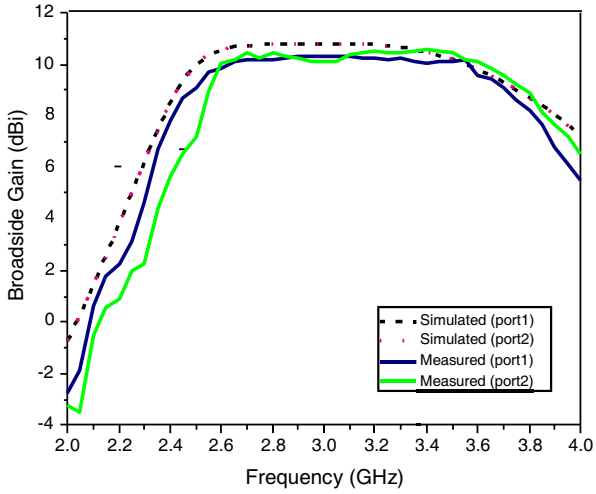

Figure 24. Comparison of simulated and measured broadside gain of the antenna from port 1 and port 2.

Table 2. The comparison between simulated and measurements results.

	Port 1 (Simulated)	**Port 1 (Measured)**	**Port 2 (Simulated)**	**Port 2 (Measured)**
−10 dB Bandwidth	32.25% (2.6–3.6 GHz)	34.37% (2.65–3.75 GHz)	32.25% (2.6–3.6 GHz)	34.21% (2.63–3.67 GHz)
−15 dB Bandwidth	18.8% (2.75–3.32 GHz)	15.38% (2.7–3.15 GHz)	18.8% (2.75–3.32 GHz)	19.8% (2.82–3.44 GHz)
Bandwidth (isolation > 20 dB)	18.2% (2.75–3.3 GHz)	25.39% (2.75–3.55 GHz)	18.2% (2.75–3.3 GHz)	25.39% (2.75–3.55 GHz)
Bandwidth (Isolation > 15 dB)	36.2% (2.6–3.75 GHz)	30.44% (2.65–3.6 GHz)	36.2% (2.6–3.75 GHz)	30.44% (2.65–3.6 GHz)
Broadside Gain for (−10 dB Bandwidth)	(10.7–11 dBi)	(10.2–10.4 dBi)	(10.7–11 dBi)	(10.25–10.52 dBi)

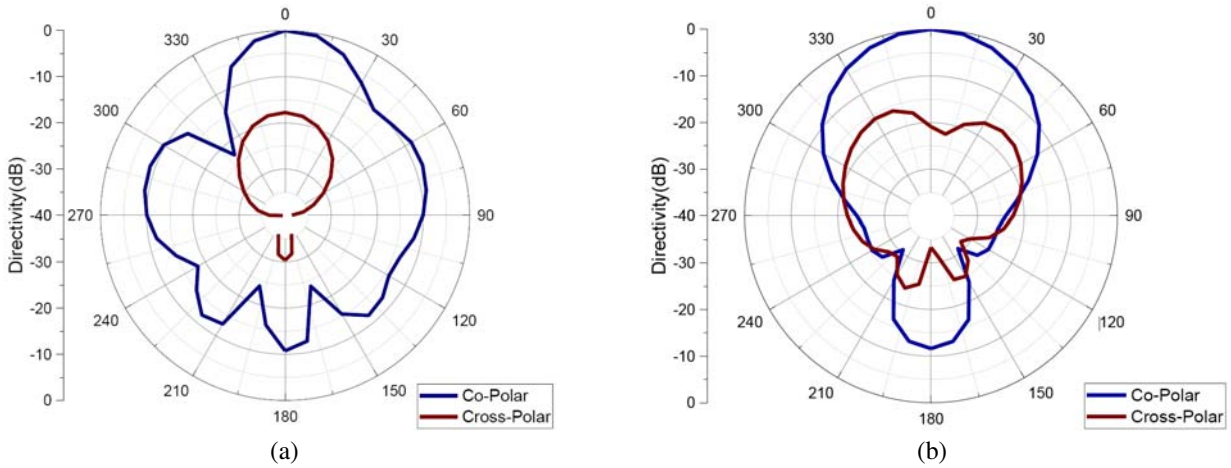

Figure 25. Simulated co-polarization and cross-polarization from port 1 at 2.6 GHz. (a) XZ plane, (b) YZ plane.

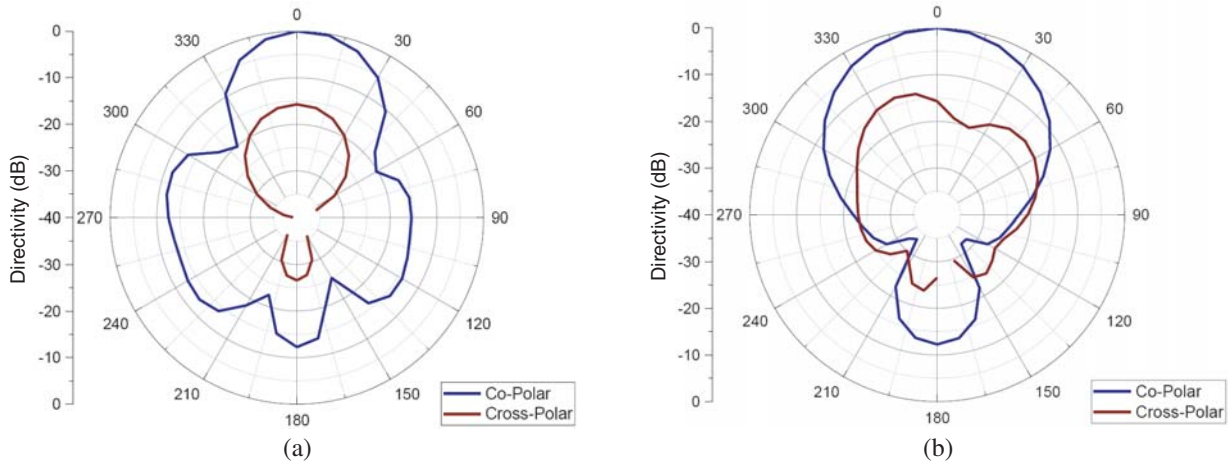

Figure 26. Simulated co-polarization and cross-polarization from port 1 at 2.9 GHz. (a) XZ plane, (b) YZ plane.

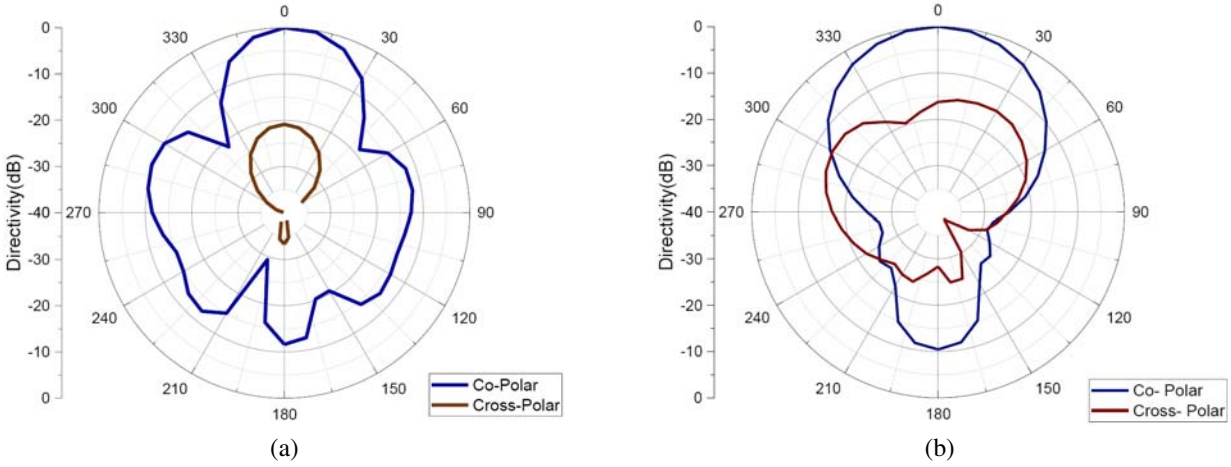

Figure 27. Simulated co-polarization and cross-polarization from port 1 at 3.4 GHz. (a) XZ plane, (b) YZ plane.

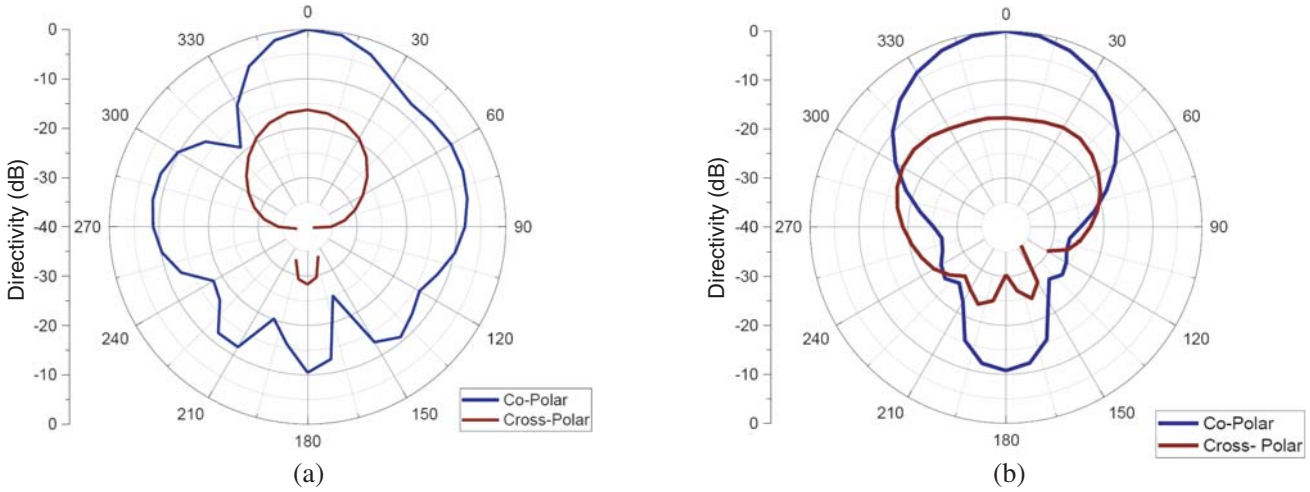

Figure 28. Simulated co-polarization and cross-polarization from port 1 at 3.6 GHz. (a) XZ plane, (b) YZ plane.

Table 3. Comparison of the proposed dual polarized antenna from antenna reported in the references.

REF	Total planner area & Total height	-10dB/-15dB Impedance bandwidth	Peak Gain ,1 dB Gain bandwidth & Cross-Polarization	Impedance Bandwidth Isolation>15dB & >20dB	Feeding Technology	Technology	Components used in the Fabrication
[9]	$0.67\lambda^2$ & 0.075λ	20.4% / 8.9%	8 dBi , 16.67 % & Below 20 dB at center frequency	20.4 % & 20.4 %	2-baluns feedings	Patch antenna with baluns	3 FR 4 substrates, T shape slot, folded microstrip line, Printed baluns feeding network, bow tie slots.
[12]	$3.61\lambda^2$ & 0.53λ	89% / 75%	8.7dBi , 60.8 % & Below 25 dB	89 % /89%	4 baluns feedings	Shorted dipole & baluns	4 printed dipoles, crossfeed lines, reflector, 4 spacers, 4 integrated baluns, 2 coaxial cables,2 SMA connector, Rogers 4003C substrates
[13]	$3.61\lambda^2$ & 0.64λ	16.5%/14.8%	15.5 dBi , 16.4 % & Below 20 dB	16.5 % & 16.5 %	2-Microstrip line	**FPA** with **PRS**	4 layer-dielectric substrates, 8×8 PRS quad layer cell, **DRA**,
[14]	$1.16\lambda^2$ & 0.24λ	70 % /NA	9.5 dBi, 35% & Below 25 dB	70 % & 70%	Commonly Fed	Commonly-fed Microstrip antenna	Power divider, resisters, baluns, FR4 substrates, Reflector,4 staircase loops
[15]	$2.16\lambda^2$ & 0.14λ	45.4% /28.5%	8.4 dBi , 45.4% & Below 20 dB	45.4% &45.4 %	4 probe with $2, 180^0$ baluns	Patch antenna with the metallic slot.	2 wideband baluns, 4 U shape probe, 4-slot group, metallic ground wall.
This work	$2.01\lambda^2$ & 0.24λ	34.21%/15.38%	10.52 dBi, 40.6%, & Below 15 dB entire bandwidth.	30.4% & 25.4%	2-Coaxial probe	Suspended cylinder & shorting strips	2 cylinder, 2 strips, a ground plane

FPA- Fabray Perot antenna, **PRS**- partially reflective surface, **DRA**- Dielectric resonator antenna, λ- wavelength at the center frequency.

from port 1 and 34.21% (2.63–3.67 GHz) measured from port 2. The simulated isolation between the ports is more than 15 dB for 36.2% (2.6–3.75 GHz); however, 30.44% (2.65–3.6 GHz) is measured from the prototype. The broadside gain of the proposed antenna is 10.8 ± 0.1 dBi over -10 dB impedance bandwidth; however, broadside gain of 10.2–10.4 dBi is measured from port 1 and 10.25–10.52 dBi measured from port 2. Therefore, small deviation of the measurement from simulated results is attributed to the fabrication tolerances and measurements errors. The co-polarization and cross-polarization components of the antenna are simulated in XZ and YZ planes at different frequencies over -10 dB impedance bandwidth which is shown in Figures 25–28, and results show that the cross-polarized

component is below 15 dB with respect to the co-polarized component in the broadside direction in both XZ and YZ planes. The front to back ratio is more than 10 dB over the entire impedance bandwidth in both planes. In Table 3, the performance of the proposed antenna is compared to the antennas reported in the references, and the proposed antenna uses fewer components. Simple coaxial feeding is used for excitation; therefore, the fabrication cost is low.

7. CONCLUSION

The paper presents a low-cost high gain dual polarized antenna with suspended cylinder and ground connected cylinder geometry for base station applications. The antenna structure is simple, and fabrication requires 2 cylinder, 2 shorting strips, and a circular ground plane. All these components are designed by a copper sheet of thickness 0.4 mm. The antenna is fed from two orthogonal diameters of the cylinders from 2 coaxial probes; therefore, no external feeding networks are required. Only metal is used for fabrication of this antenna; therefore, power handling capacity of the antenna is high as compared to the dielectric and microstrip antennas [16]. The measurement results show that the antenna has -10 dB impedance 34.37% (2.65–3.75 GHz) when it is measured from port 1 and 34.21% (2.63–3.67 GHz) when it is measured from port 2. The measured isolation between ports is more than 15 dB for 30.44% (2.65–3.6 GHz) and more than 20 dB for 25.39% (2.75–3.55 GHz). The simulated antenna has a symmetrical response with respect to the ports. However, the measurements results slightly deviate due to fabrication tolerances and measurement errors. The antenna has a stable broadside radiation pattern, and 10.2–10.4 dBi broadside gain is measured at port 1 and 10.25–10.52 dBi broadside gain measured at port 2 over the entire -10 dB impedance bandwidth. The resonance frequency of the proposed antenna is tunable with width of the shorting strips. The antenna has characteristics such as low cost, dual polarizations, broadband, high gain, flat gain, stable radiation pattern, tunable, high power handling capacity, simple coaxial feeding, simple metallic structure, and fabrication exclusively with metal. All these characteristics of this antenna will make it more attractive for wireless communications.

REFERENCES

1. Balanis, C. A., *Antenna Theory: Analysis and Design*, 3rd Edition, 2–3, John Wiley & Sons, New York, 2011.
2. Sun, K., D. Yang, Y. Chen, and S. Liu, "A broadband commonly fed dual-polarized antenna," *IEEE Antennas and Wireless Propagation Letter*, Vol. 17, No. 5, May 2018.
3. Cheng, Y., Y. Li, and W. Lu, "A novel compact dual-polarized antenna," *International Journal of Antennas and Propagation*, Vol. 2016, Article ID 6304356, 5 pages, 2016.
4. Lian, R., Z. Wang, Y. Yin, J. Wu, and X. Song, "Design of a low-profile dual-polarized stepped slot antenna array for base station," *IEEE Antennas and Wireless Propagation Letters*, Vol. 15, 2016.
5. Luo, Y. and Q. X. Chu, "Oriental crown-shaped differentially fed dual polarized multipole antenna," *IEEE Trans. Antennas Propag.*, Vol. 63, No. 11, 4678–4685, November 2015.
6. Yu, J., Y. Sun, H. Zhu, F. Li, and Y. Fang, "Stacked-patch dual-band & dual-polarized antenna with broadband baluns for WiMAX & WLAN applications," *Progress In Electromagnetics Research M*, Vol. 68, 41–52, 2018.
7. Secmen, M. and A. Hizal, "A dual-polarized wideband patch antenna for indoor mobile communications applications," *Progress in Electromagnetics Research*, Vol. 100, 189–200, 2010.
8. Cui, G.-F., S.-G. Zhou, S.-X. Gong, and Y. Liu, "A compact dual-polarized antenna for base station application," *Progress In Electromagnetics Research Letters*, Vol. 59, 7–13, 2016.
9. Deng, C., Y. Li, Z. Zhang, and Z. Feng, "A wideband high-isolated dual-polarized patch antenna using two different balun feedings," *IEEE Antennas and Wireless Propagations Letters*, Vol. 13, 2014.
10. Yu, J., Y. Sun, H. Zhu, F. Li, and Y. Fang, "Stacked-patch dual-band & dual-polarized antenna with broadband baluns for WiMAX & WLAN applications," *Progress In Electromagnetics Research M*, Vol. 68, 41–52, 2018.

11. Huang, H., Y. Liu, and S. Gong, "Broadband dual-polarized omnidirectional antenna for 2G/3G/LTE/WiFi applications," *IEEE Antennas and Wireless Propagations Letters*, Vol. 15, 2016.
12. Wen, L.-H., S. Gao, C.-X. Mao, Q. Luo, W. Hu, Y. Yin, and X. Yang, "Wideband dual-polarized antenna using shorted dipoles," *IEEE Access*, Vol. 5, 2018.
13. Qin, P.-Y., L.-Y. Ji, S.-L. Chen, and Y. J. Guo, "Dual-polarized wideband Fabry-Perot antenna with quad-layer partially reflective surface," *IEEE Antennas and Wireless Propagation Letters*, Vol. 17, No. 4, April 2018.
14. Sun, K., D. Yang, Y. Chen, and S. Liu, "A broadband commonly fed dual-polarized antenna," *IEEE Antennas and Wireless Propagation Letters*, Vol. 17, No. 5, May 2018.
15. Li, Q., S. W. Cheung, and C. Zhou, "A low-profile dual-polarized patch antenna with stable radiation pattern using ground-slot groups and metallic ground wall," *IEEE Transactions on Antennas and Propagation*, Vol. 65, No. 10, October 2017.
16. Yadav, S. C. and S. P. Duttagupta, "Novel broadband high gain antenna design by the suspended cylinder and shorting pin," *Progress In Electromagnetics Research C*, Vol. 86, 247–256, September 2018.